



## Full Length Article

# Establishment and verification of a metering scheme for biomass-coal blending ratios based on $^{14}\text{C}$ determination

Yinchen Wang<sup>a</sup>, Zhongyang Luo<sup>a,\*</sup>, Yuxing Tang<sup>a</sup>, Qinhui Wang<sup>a</sup>, Chunjiang Yu<sup>a</sup>,  
Xudong Yang<sup>a</sup>, Qianyuan Chen<sup>b</sup>

<sup>a</sup> State Key Laboratory of Clean Energy Utilization, Zhejiang University, Zhada Road 38, Hangzhou 310027, China

<sup>b</sup> Institute of Modern Physics, Fudan University, Shanghai 200433, China



## ARTICLE INFO

## Keywords:

$^{14}\text{C}$  method  
Radiocarbon  
Co-combustion  
Biomass-coal blending ratio  
Industrial power plant

## ABSTRACT

The lack of reliable schemes for measuring biomass-coal blending ratios hinders the development of biomass-coal co-combustion. In this study, the accuracy and sensitivity of the  $^{14}\text{C}$  method were verified on a free-fall reactor with blending ratios of 0.99 ~ 10.93%. Comparison between accelerator mass spectrometry (AMS)-graphitization and liquid scintillation counting (LSC)-benzene synthesis was performed in terms of accuracy, precision and costs. Based on these, a complete scheme for measuring the blending ratios in industrial power plants was established and applied in a power plant for verification. The results on the free-fall reactor perfectly agreed with actual ratios (less than 0.43%, 5.69% of absolute and relative errors); LSC with higher cost-effectiveness was capable of measuring the blending ratios accurately. Blending ratios less than 3% in the power plant were accurately measured with the established scheme (less than 0.22%, 10.68% of absolute and relative errors). Factors affecting the accuracy, especially the  $^{14}\text{CO}_2$  contamination, should be considered for improvement of the accuracy.

## 1. Introduction

Rapidly developing society and increasingly dense populations have raised the levels of  $\text{CO}_2$ , the main greenhouse gases, and other hazardous gases such as  $\text{NO}$ ,  $\text{SO}_2$ . A huge challenge has fallen on the road to achieving ‘carbon neutrality’ and ‘carbon peaking’ [1].

Biomass energy plays an indispensable role in accomplishing sustainable development due to its renewability, cleanability and carbon-neutrality [2,3]. However, the current power generation from biomass energy is far less than that from fossil energy, which is attributed to many obstacles of the major utilization of biomass (direct combustion), such as corrosion [4] and deposition [5] occurring in boilers. Biomass co-combustion with coal can not only solve the corrosion deposition caused by the high content of alkali metals, but also partly provide a fuel alternative to coal, therefore, it is perceived to be a promising biomass utilization approach [6,7]. The governments of many countries have implemented financial subsidies to encourage power plants to utilize biomass energy as the partly substitute for coal. The more biomass they use, the more financial subsidies they get. Thus, a reliable and accurate monitoring tools for the biomass-coal blending ratios is urgently needed.

The  $^{14}\text{C}$ -based method was first applied to archaeology, calculating the ages of antiques according to their  $^{14}\text{C}$  activities and negative exponential decay law of radioactive carbon [8]. Afterwards, the  $^{14}\text{C}$  method worked in the quantification of biogenic fractions of various materials, which is based on the principle that biogenic and fossil fractions significantly differ in the  $^{14}\text{C}$  values. Fossil carbon sources have been decayed out due to their ages which are far larger than the half-life of radiocarbon (5730 years). But biogenic carbon sources contain well measurable  $^{14}\text{C}$  values which are equal to those of atmospheric  $\text{CO}_2$ . Consequently,  $^{14}\text{C}$  activities of materials should be the results of the combined effect of two kinds of carbon that differently originated. Previous studies have accentuated the calculation of the biogenic fractions of plastics [9], foam [10] and some other manufactured products [11].

Recently the  $^{14}\text{C}$  method has been considered as the backbone for measuring biogenic composition in the industry, especially in waste incineration plants. Hämäläinen et al. [12] pioneered the investigation on  $^{14}\text{C}$  activities in the flue gas  $\text{CO}_2$  samples in power plants located in Finland, followed by [13,14] calculating the biogenic fractions of combusted waste in industrial plants. The consistency of biogenic

\* Corresponding author.

E-mail address: [zyluo@zju.edu.cn](mailto:zyluo@zju.edu.cn) (Z. Luo).

<https://doi.org/10.1016/j.fuel.2022.125198>

Received 16 November 2021; Received in revised form 22 June 2022; Accepted 4 July 2022

Available online 11 July 2022

0016-2361/© 2022 Elsevier Ltd. All rights reserved.

fractions calculated based on the  $^{14}\text{C}$  method and mass data method has been explored by [15]. Based on the certification of the suitability of the  $^{14}\text{C}$  method applied in industrial plants, factors affecting the accuracy of the  $^{14}\text{C}$  method, including the contamination caused by NaOH solution [16], the reference of  $^{14}\text{C}$  content of pure biomass [17] and the best sampling period [18,19], have gradually been explored.

As above mentioned, the  $^{14}\text{C}$  method is a reliable tool for calculating the biogenic fractions in waste incineration plants. In addition, based on the same principle, the  $^{14}\text{C}$  method can accurately measure the blending ratios of biomass when it is co-combusted with fossil fuel such as coal, petroleum and natural gas, almost all of which, however, were mostly concerned with bio oil-petroleum fuel [20,21] and biogas-natural gas fuel [22]. Surprisingly, very little has been finished concerning biomass-coal fuel, and even though where such study exists [23], it has not been extended to industrial plants for verification. Additionally, there are adequate studies on the  $^{14}\text{C}$  method focusing on the utilization of accelerator mass spectrometry (AMS) [24,25] with high economic costs, but scarce on the utilization of liquid scintillation counter (LSC) [26] which is more cost-effective.

As reported in a comprehensive review on biomass co-combustion with coal [27], considerable progress has been made in the field of co-combustion. However, one of the most urgent works is to establish a reliable and economic scheme for metering the biomass blending ratios when it is co-combusted with coal. High accuracy and high cost-effectiveness are the important requirements of a suitable metering scheme. Therefore, it is imperative to present and test a scheme for calculating the biomass-coal blending ratios that can be applied in the industry. More importantly, a comprehensive comparison between AMS and LSC, the two main  $^{14}\text{C}$  analysis methods at present, should be considered.

In this study, the accuracy and reliability of the  $^{14}\text{C}$  method applied in the calculation of biomass-coal blending ratios and the comparison between AMS and LSC were sufficiently explored on a free-fall reactor experimental equipment in the laboratory. The results were used to establish a complete scheme for metering biomass-coal blending ratios suitable for industrial power plants, and then, for verification, it was applied in a biomass gasification coupled with coal combustion power plant located in Hubei, China. Moreover, the potential factors which may affect the accuracy of the scheme were analyzed in detail. Besides the establishment of a metering scheme for biomass-coal blending ratios, the results of this study contribute to the future development of large-scale utilization of co-combustion to some extent.

## 2. Materials and methods

### 2.1. Free-fall reactor experimental equipment

#### 2.1.1. Materials

Paw sawdust (PS), corn straw (CS) and three kinds of coal with different degrees of coalification including Shenmu coal (SMC), Zhundong coal (ZDC) and Changzhi coal (CZC) were used as feedstocks for the co-combustion. After being dried at 105 °C for 10 h, the raw materials were pulverized to less than 106  $\mu\text{m}$  and divided into different groups according to the mass mixing ratios, as shown in Table 1.

#### 2.1.2. Experimental equipment and procedures

The experiments were performed at micro-positive pressure to prevent gas leakage, with high purity air as the combustion agent, in a free-fall reactor which has the basic structure shown in Fig. 1. The experimental setup consists of a combustion chamber, a material feeder, a pneumatic system, a purification-absorption system and a cooling system.

A corundum pipe was employed as the reactor for combustion. Its inner diameter and total length were 85 mm, 2300 mm, respectively. It contained a thermostatic area of 1800 mm heated by three silicon-carbon rods. The operational temperature was controlled at 1100 °C.

**Table 1**

Materials groups with different materials or blending ratios.

| Sample name | Materials |      | $f_{biomass}^{mb}$ [%] | Remark      |
|-------------|-----------|------|------------------------|-------------|
|             | Biomass   | Coal |                        |             |
| FFR-1       | –         | SMC  | 0.00                   | Single fuel |
| FFR-2       | –         | ZDC  |                        |             |
| FFR-3       | –         | CZC  |                        |             |
| FFR-4       | PS        | –    | 100.00                 | Mixed fuel  |
| FFR-5       | CS        | –    |                        |             |
| FFR-6       | PS        | CZC  | 5.00                   |             |
| FFR-7       |           | CZC  | 9.97                   |             |
| FFR-8       |           | SMC  | 9.97                   |             |
| FFR-9       |           | ZDC  | 10.06                  |             |
| FFR-10      | CS        | CZC  | 10.03                  |             |
| FFR-11      |           | SMC  | 10.09                  |             |
| FFR-12      |           | SMC  | 1.01                   |             |

The materials were fed into the reactor by a syringe feeder under gravity with a speed of 1 g min<sup>-1</sup>. For safety reasons, an air-cooled chiller was used to cool the top and the bottom of the chamber. The basic performance, such as concentricity, sealing, and temperature field, were tested before experiments.

Firstly, high purity air was imported into the reactor while the feedstocks were simultaneously loaded into the feeder. Then the materials feeder began to operate and the materials travelled through the reactor while combusting. During operation, the flue gas exited the reactor, and then passed through a filter, a vacuum pump, and a flowmeter. Lastly, the carbon dioxide in the gas was absorbed by the sodium hydroxide solution and simultaneously analyzed by the HORIBA PG-350 flue gas analyzer for gas composition to ensure the CO content was slim, representing almost all combusted carbon were converted to CO<sub>2</sub>. After combustion for about 30 min, the ash falling on the bottom of the reactor was collected and the CO<sub>2</sub> absorbed by the NaOH was converted into strontium carbonate with the method mentioned in Ref. [23].

#### 2.1.3. $^{14}\text{C}$ determination

To determine the  $^{14}\text{C}$  activity a high-vacuum benzene synthesis system was built [23] and following the work of Ref. [28], a multi-functional graphitization system was also built. Each SrCO<sub>3</sub> sample originating from the combustion flue gas was prepared into benzene before it was detected by a liquid scintillation counter (LSC, PE Quantuland 1220), meanwhile each SrCO<sub>3</sub> sample was graphitized before it was analyzed by an accelerator mass spectrometer (AMS). By convention [29],  $^{14}\text{A}$ , the so-called  $^{14}\text{C}$  activity, is defined as the  $^{14}\text{C}/^{12}\text{C}$  ratio of a sample to the  $^{14}\text{C}/^{12}\text{C}$  ratio of the standardized oxalic acid samples (OXII). For convenience, the  $^{14}\text{C}$  activities of the samples are denoted by 'A' with some footnotes in this paper.

#### 2.1.4. Calculation of the carbon-based blending ratios

The  $^{14}\text{C}$  activity of CO<sub>2</sub> from the flue gas ( $A_{fluegas}$ ) is determined by the proportion of CO<sub>2</sub> from different sources in the flue gas ( $f_x^{cb}$ ) and their own  $A_{fluegas}$  value, with the superscript 'cb' referring to the proportion based on the mass of carbon:

$$A_{fluegas} = f_{biomass}^{cb} \times A_{biomass} + f_{coal}^{cb} \times A_{coal} + f_{air}^{cb} \times A_{air} + f_{NaOH}^{cb} \times A_{NaOH} \quad (1)$$

The CO<sub>2</sub> source can be divided into: (1) CO<sub>2</sub> from the biomass ( $f_{biomass}^{cb}$ ), (2) CO<sub>2</sub> from the coal ( $f_{coal}^{cb}$ ), (3) CO<sub>2</sub> present in the air used as the fueling agent and ends up in the emitted flue gas ( $f_{air}^{cb}$ ), (4) CO<sub>2</sub> originating from the air and dissolved in the NaOH ( $f_{NaOH}^{cb}$ ). Regardless of the coal type, its formed age is larger than 5730 years (the half-life of  $^{14}\text{C}$ ), therefore, the radioactive carbon in the coal has completely decayed. The combustion agent containing 79% nitrogen and 21% oxygen from the gas cylinder could be excluded from the interference of the  $^{14}\text{CO}_2$  in the air. Hence, Eq. (2) can be written as:

$$f_{biomass}^{cb} = (A_{fluegas} - A_{NaOH} \times f_{NaOH}^{cb}) / A_{biomass} \times 100\% \quad (2)$$

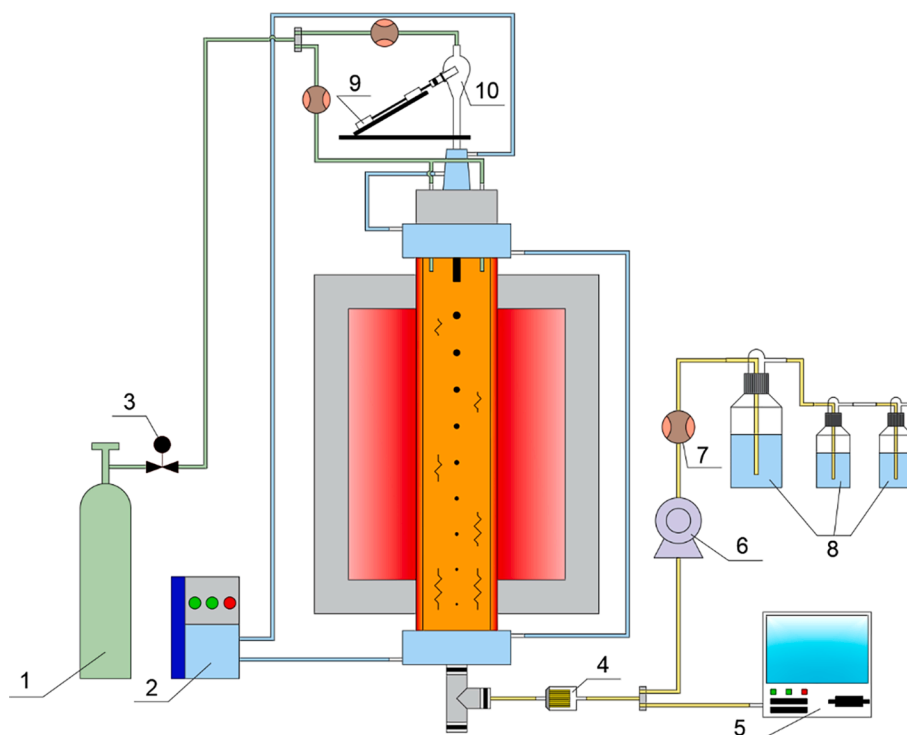


**Fig. 1.** Schematic diagram of the free-fall reactor for biomass-coal co-combustion. 1: High-purity air; 2: Air-cooled chillers; 3: Valve; 4: Filter; 5: HORIBA PG-350 flue gas analyzer; 6: Vacuum pump; 7: Flowmeter; 8: 2.5 mol L<sup>-1</sup> NaOH solution; 9: Syringe materials feeder; 10: Funnel.

A reference of ‘ $A_{biomass}$ ’,  $1.130 \pm 0.038$ , representing the <sup>14</sup>C activity of pure biogenic waste, was proposed by [17]. In contrast, this study focused on the determination of the biomass blending ratios during co-firing with coal, so that the biogenic materials in this study is concrete rather than non-concrete in the waste. The ‘ $A_{fluegas}$ ’ of single fuel groups represent the <sup>14</sup>C activity of this biomass.

It is worth noting that we cannot calculate the actual biomass carbon-based blending ratios simply based on the mass-based ratios ( $f_{biomass}^{mb}$ ,  $f_{coal}^{mb}$ ) and the organic carbon content of the raw materials ( $C_{biomass}$ ,  $C_{coal}$ ) because although the biomass is easy to completely burn in the reactor, coal ash usually contains a small amount of unburned carbon ‘ $C_{loss}$ ’ (%). According to Eq. (2), the calculated biomass-coal blending ratios are related to the coal whose carbon ends up as the CO<sub>2</sub> in flue gas, i.e., which is completely burned, not related to the coal which is incompletely burned, thus, the actual values of those can be quantified by this equation:

$$f_{biomass}^{cb\_actual} = \frac{(f_{biomass}^{mb} \times C_{biomass}) / [f_{biomass}^{mb} \times C_{biomass} + (1 - f_{biomass}^{mb}) \times C_{coal} \times (1 - C_{loss})]}{(f_{biomass}^{mb} \times C_{biomass}) / [f_{biomass}^{mb} \times C_{biomass} + (1 - f_{biomass}^{mb}) \times C_{coal} \times (1 - C_{loss})]} \quad (3)$$

## 2.2. The industrial power plant

### 2.2.1. Fuel and facilities

The power plant we selected for the verification of the <sup>14</sup>C method in the calculation of biomass blending ratios is located in Hubei, China. Field sampling was executed from March 21, 2021 to March 24, 2021. A circulating fluidized bed boiler was utilized for biomass gasification and the generated biogas was imported into a 640 MW pulverized coal furnace for combustion together with anthracite coal from six coal mills. According to the distributed control system (DCS), there were four different ratios of coal from six coal feeders. These four kinds of mixing coal (Coal 1,2,3,4) and three kinds of biomass used as gasification feedstocks including rice husk (RH), corn straw (CS) and black wood residue (BWR) were brought back to the laboratory for industrial,

elemental analysis, and <sup>14</sup>C determination.

### 2.2.2. Sampling and sample preparation

Sampling in power plants should follow the principle of not affecting the normal operation, so it's impossible to freely choose the biomass-coal blending ratios. The CO<sub>2</sub> in flue gas from six operation conditions, with different biomass or different blending ratios, was sampled during four days. When the flue gas from the combustion of biomass gas and pulverized coal travelled through the air preheater, it was sucked out by a 100 mm sampling gun with reheat apparatus preventing water vapor condensation in the gun-body. The vapor in the flue gas was removed by a 2 °C condenser at the end of the gun. The CO<sub>2</sub> in the flue gas, without particle, with a constant flow of 4 L min<sup>-1</sup> controlled by a flowmeter, was absorbed when passing through two washing bottles, each filled with 2.5 mol L<sup>-1</sup> sodium hydroxide solution. The composition of the flue gas was detected by the LaoYing 3012H flue gas analyzer which was arranged in a branch circuit in parallel with two absorption bottles. After a sampling period of one hour, the dissolved CO<sub>2</sub> was converted into SrCO<sub>3</sub> by the same method in Section 2.1.2. The operating-sampling system is shown in Fig. 2.

The CO<sub>2</sub> originally existed in the atmosphere for combustion and ended in flue gas shares about 0.25% of the total CO<sub>2</sub> in the flue gas [15]. In order to solve the “contamination” caused by this part of CO<sub>2</sub>, a synchronized atmosphere sampling system was adopted. A constant flow of 4 L min<sup>-1</sup> was controlled by a diaphragm pump followed by two washing bottles full of 1 mol L<sup>-1</sup> NaOH placed at the blower inlet. In the same way, the ambient CO<sub>2</sub> ended up in the form of SrCO<sub>3</sub>.

The calculated biomass-coal blending ratios by the <sup>14</sup>C method is related to the fuel combusted completely, in other words the carbon converted to CO<sub>2</sub>, but not in the ash. In order that the biomass blending ratios related to all fuel, whether completely burned or not, could be extrapolated by the results quantified by the <sup>14</sup>C method, another synchronized work (ash and slag collecting) was performed. The carbon content of the ash and the slag could be obtained by thermogravimetric analysis.

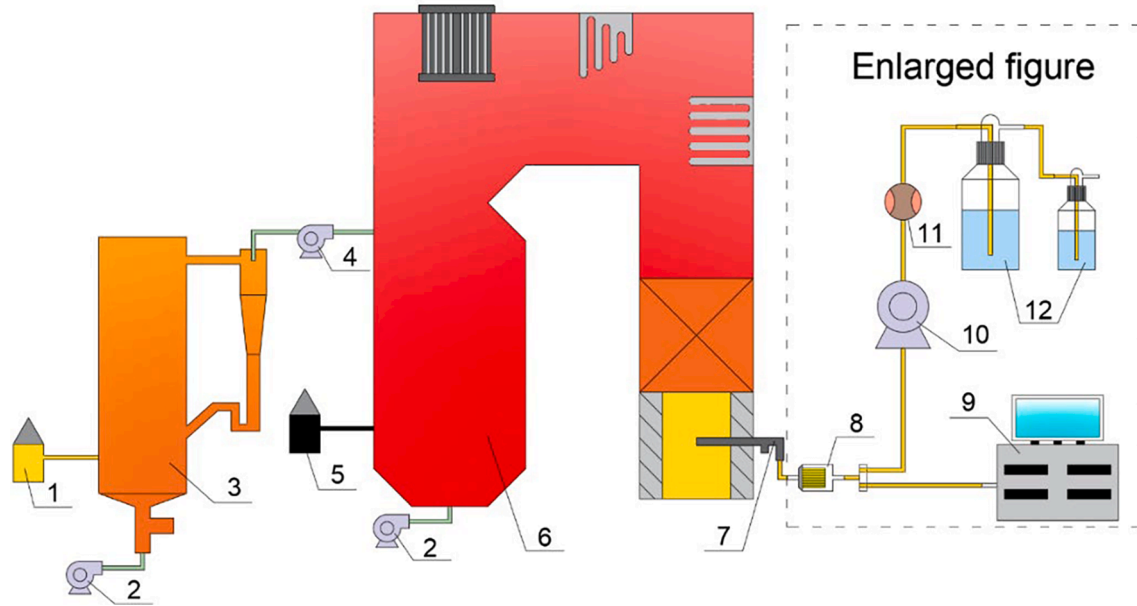


**Fig. 2.** Schematic diagram of the biomass coal co-combustion power plant and the sampling system. 1: Biomass warehouse; 2: Blower; 3: Biomass gasifier; 4: Blower; 5: Coal warehouse; 6: Pulverized coal furnace; 7: Sampling gun; 8: Filter; 9: LaoYing 3012H flue gas analyzer; 10: Vacuum pump; 11: Flowmeter; 12: 2.5 mol L<sup>-1</sup> NaOH solution.

### 2.2.3. <sup>14</sup>C determination

The biomass samples were graphitized before being analyzed by an AMS. The six flue gas CO<sub>2</sub> samples were synthesized as benzene before being determined by the Quantulant 1220 LSC, and four of them were also determined by AMS to make a comparison with the LSC results. Since the atmospheric <sup>14</sup>C activity varies only slightly over a short period, the six SrCO<sub>3</sub> samples converted from ambient CO<sub>2</sub> were sampled in equal amounts before being detected by AMS.

### 2.2.4. Calculation of the biomass-coal blending ratios

In this section, a complete scheme that can be applied in industrial power plants is presented in detail. This scheme follows the same principle as the experiments performed in the laboratory mentioned in Section 2.1.4. However, the fraction of ambient CO<sub>2</sub> must be considered and the biomass fuel is not the single fuel but mixed fuel:

$$f_{biomass}^{cb} = [A_{fluegas} - (A_{air} \times f_{air}^{cb} + A_{NaOH} \times f_{NaOH}^{cb})] / \sum_{i=1}^n (A_{bio-x} \times f_{bio-x}^{cb}) \times 100\% \quad (4)$$

In power plants, the ultimate goal of the utilization of biomass and coal is to generate electricity by the released heat, so calculating the biomass blending ratio  $f_{biomass}^{cb}$ , based on the energy contributing to electricity generation is meaningful. For the calculation of the energy-based blending ratios, the low heat values of biomass gas and coal ( $h_{biogas}$ ,  $h_{coal}$ ) and the organic carbon content ( $C_{biogas}$ ,  $C_{coal}$ ) are needed as the necessary parameters for the quantification of  $HC_{biomassorcoal}$ , which represents the heat generation per unit mass of carbon. The carbon content of biomass gas is correlated with the gas composition. Considering the heat loss in the boiler, the values of  $q_1$ – $q_6$  are also needed. There is no heat loss ( $q_4$ ,  $q_6$ ), from incomplete combustion of solids and ash emissions, for biomass because it was combusted in the form of biomass gas:

$$HC_{biomass} = [h_{biogas} \times (1 - q_2 - q_3 - q_5)] / C_{biogas} \quad (5)$$

$$HC_{coal} = [h_{coal} \times (1 - q_2 - q_3 - q_4 - q_5 - q_6)] / C_{coal} \quad (6)$$

All these key parameters were obtained from the distributed control system. The energy-based biomass blending ratio  $f_{biomass}^{cb}$ , could be calculated by the equation as follows:

$$f_{biomass}^{cb} = (HC_{biomass} \times f_{biomass}^{cb}) / [HC_{biomass} \times f_{biomass}^{cb} + HC_{coal} \times (1 - f_{biomass}^{cb})] \times 100\% \quad (7)$$

## 3. Results and discussion

### 3.1. Free-fall reactor experimental equipment

Herein, the calculated biomass-coal blending ratios carried out on the free-fall reactor system are presented. The calculated values of blending ratios based on the <sup>14</sup>C determination shows a good linearity with the actual values.

#### 3.1.1. The key parameters of the <sup>14</sup>C method

Table 2 shows the key parameters, including  $A_{fluegas}$ ,  $A_{biomass}$ , which were both detected by AMS and LSC, and  $A_{NaOH} \times f_{NaOH}^{cb}$ , of the <sup>14</sup>C method on the free-fall reactor experimental equipment. Since the <sup>14</sup>C in the coal is completely decayed, the contamination caused by ambient CO<sub>2</sub>, as mentioned in Eq. (2), was approximated by the average of the  $A_{fluegas}$  of three classes of coal, whose sources could only be the atmospheric CO<sub>2</sub> absorbed by NaOH.

The test results of AMS and LSC showed that the <sup>14</sup>C activity of PS (perennial plants) was significantly higher than CS (annual plants). This might be due to the fact that the atmospheric <sup>14</sup>C activity decreased year by year attributed to the application of fossil fuel (Suess effect) [30]. Moreover, the <sup>14</sup>C activities of plants, which vary with the atmospheric <sup>14</sup>C activity, are close but not the same as the atmosphere, and they are also decided by various factors such as planting time, harvest time, surrounding fossil carbon source emissions, etc [31]. To improve the accuracy, sampling and <sup>14</sup>C measurement of the biomass fuel in power plants are recommended. Norton et al. [11] pointed out the reasonable absolute uncertainty of LSC when it was used to detect pure biomass was about 3% and the results of our study were consistent with this result. Despite the higher uncertainty of LSC than that of AMS, the test values for both were approximately identical and the AMS results were within the uncertainty ranges of LSC results.

Because the <sup>14</sup>C activity of the coal is zero, the higher the carbon

**Table 2**  
The key parameters of the  $^{14}\text{C}$  method on the free-fall reactor experimental equipment.

| Sample name | Mixed Fuel |      | $A_{\text{fluegas}}$ [pMC] |                       | $A_{\text{biomass}}$ [pMC] |                       | $A_{\text{NaOH}} \times f_{\text{NaOH}}^{\text{cb}}$ [pMC] |
|-------------|------------|------|----------------------------|-----------------------|----------------------------|-----------------------|--|
|             | Biomass    | Coal | AMS-Graphitization         | LSC-Benzene Synthesis | AMS-Graphitization         | LSC-Benzene Synthesis |  |
| FFR-6       | PS         | CZC  | –                          | 4.57 ± 0.24           | 110.12 ± 0.4               | 110.08 ± 4.63         | 0.19 ± 0.06  |
| FFR-7       |            | CZC  | 10.16 ± 0.07               | 10.20 ± 0.42          |                            |                       |  |
| FFR-8       |            | SMC  | 11.76 ± 0.07               | 11.86 ± 0.40          |                            |                       |  |
| FFR-9       |            | ZDC  | 9.26 ± 0.06                | 8.70 ± 0.43           |                            |                       |  |
| FFR-10      | CS         | CZC  | 8.60 ± 0.06                | 8.29 ± 0.44           | 103.11 ± 0.38              | 103.11 ± 4.2          |  |
| FFR-11      |            | SMC  | –                          | 11.00 ± 0.34          |                            |                       |  |
| FFR-12      |            | SMC  | –                          | 1.32 ± 0.18           |                            |                       |  |

content of the coal is, the lower the  $^{14}\text{C}$  activity of the flue gas is, when the mass-based blending ratio is close. But the Changzhi anthracite with the highest carbon content among the three types of coal deviated from this rule, which could be attributed to incomplete combustion of some carbon from the coal. This phenomenon again proves that the organic carbon in the coal didn't fully enter the flue gas, especially, for the anthracite with high fixed carbon and less activation. Therefore, the loss of the unburned carbon shouldn't be ignored when accounting for the blending ratios of biomass based on the  $^{14}\text{C}$  test results of flue gas, as given in Eq. (3).

### 3.1.2. The carbon-based blending ratios obtained by two routes

Table 3 shows the carbon-based blending ratios of biomass calculated by the  $^{14}\text{C}$  method and the corresponding actual blending ratios. The overall uncertainty (95% confidence) of  $f_{\text{biomass}}^{\text{cb}}$  was calculated from the uncertainty of  $A_{\text{fluegas}}$  and, as large contribution, the uncertainty of  $A_{\text{biomass}}$  via the laws of error propagation. To limit the cost of  $^{14}\text{C}$  measurement, only FFR7 ~ FFR10 were selected for AMS analysis, and the results of the two routes are presented in Fig. 3. Excellent agreement between AMS-graphitization and LSC-benzene synthesis was observed for these four working conditions.  $f_{\text{biomass}}^{\text{cb}}$  determined by AMS was about 0.17% higher than that obtained by LSC when the actual blending ratios varied between 7.73%~10.93%. However, the difference between the two methods was within the error bars of LSC. Based on this dataset consistency, it could be concluded that the blending ratios results obtained by the two methods following the principle of the  $^{14}\text{C}$  method are consistent even though the uncertainty of the two methods is different. It is worth mentioning that although the uncertainty of AMS is one order of magnitude smaller than that of LSC, the relative errors of AMS results are not significantly better than that of LSC. For example, the relative error of LSC was lower than that of AMS in FFR8 and FFR10. The difference between the two routes was only within the order of the magnitude of the relative error, and not much within the accuracy.

### 3.1.3. Accuracy of the $^{14}\text{C}$ method

Fig. 4 presents the fitted curves of the biomass carbon-based

**Table 3**  
The carbon-based blending ratios of biomass calculated by the  $^{14}\text{C}$  method and the corresponding actual blending ratios.

| Sample name | Mixed fuel |      | $f_{\text{biomass}}^{\text{cb}}$ based on $^{14}\text{C}$ method |                    |                       |
|-------------|------------|------|--|--------------------|-----------------------|
|             | Biomass    | Coal | $f_{\text{biomass}}^{\text{actual}}$ [%]                         | AMS-Graphitization | LSC-Benzene synthesis |
| FFR-6       | PS         | CZC  | 4.22   | –                  | 3.98 ± 0.28           |
| FFR-7       |            | CZC  | 8.87   | 9.05 ± 0.09        | 9.09 ± 0.54           |
| FFR-8       |            | SMC  | 10.93  | 10.51 ± 0.09       | 10.60 ± 0.58          |
| FFR-9       |            | ZDC  | 8.10   | 8.24 ± 0.08        | 7.73 ± 0.51           |
| FFR-10      | CS         | CZC  | 7.73   | 8.16 ± 0.09        | 7.86 ± 0.54           |
| FFR-11      |            | SMC  | 10.14  | –                  | 10.48 ± 0.54          |
| FFR-12      |            | SMC  | 0.99   | –                  | 1.10 ± 0.19           |

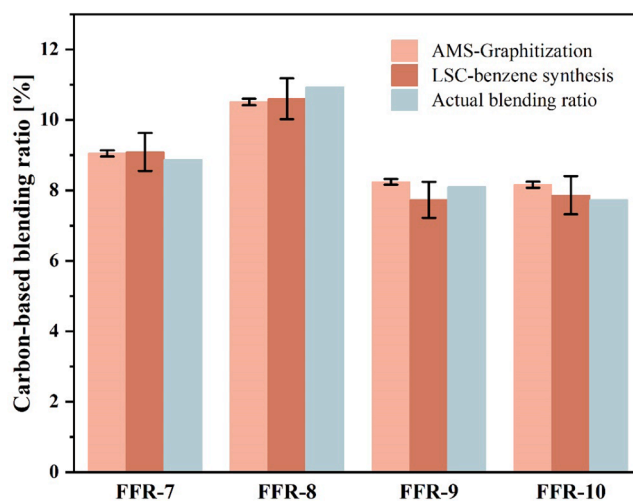


Fig. 3. The carbon-based blending ratios calculated by AMS-graphitization, LSC-benzene synthesis and the actual values.

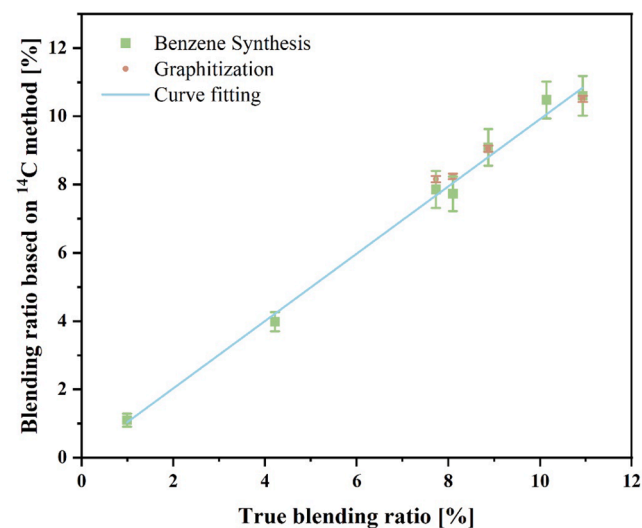


Fig. 4. The fitted curves of the biomass carbon-based blending ratios obtained by the two technical routes to the actual carbon-based blending ratios.

blending ratios obtained by the two technical routes to the actual carbon-based blending ratios. In this study,  $f_{\text{biomass}}^{\text{cb}}$  varied between 1% ~11%, and within this range the results calculated by AMS and LSC were almost the same, both with the absolute deviation from actual values less than 0.43%. The relative errors were basically below 5.69%, except for the relative error of 11.1% for the 0.99% blending ratio, but considering such a low blending ratio, the relative error of about 11% was satisfactory. The analytical equation of the fitted curve was:  $Y =$

0.9861X + 0.0563, and the value of  $R^2$  was 0.9966. Significant goodness of the fit illustrates the accuracy of the  $^{14}\text{C}$  method when it is applied in the calculation of blending ratios. The calculated results decreased or increased significantly with the decrease or increase of biomass blending ratios, thus, they showed great sensitivity. Hence, both  $^{14}\text{C}$ -based methods showed excellent accuracy and reliability.

### 3.1.4. The industrial power plant

After verifying the accuracy of the  $^{14}\text{C}$  method for biomass blending ratios metering in the laboratory, we established a complete metering scheme for biomass blending ratios and applied it in an industrial power plant located in Hubei, China. The reliability and accuracy of the scheme were approved by the great presence of results.

### 3.1.5. Operating conditions

The operating parameters including the categories of raw fuel with its corresponding ' $HC_{biomasscoal}$ ' and the running load of both gasifier and pulverized coal furnace, which were derived from the data provided by the DCS and based on the calculation method mentioned in Section 2.2.4, are presented in Table 4. IPP1-IPP4 operation conditions differed in the kinds of fuel, either biomass or coal, while IPP5-IPP6 had lower working loads than the first four which was attributed to the variation of coal feed rate leading to increased biomass blending ratios.

### 3.1.6. The key parameters of the $^{14}\text{C}$ method

The critical parameters of six operating conditions required for the  $^{14}\text{C}$ -based calculation of biomass blending ratios by Eq. (4) are shown in Table 5. To limit the cost, four representative operation conditions (IPP-1, 2, 4, 5) were selected for AMS analysis and the biomass materials of these operation conditions were RH, RH + CS, CS, and RH + BWR. The blending ratio of IPP-5 was larger than that of IPP-1,2,4.

The fractions of the  $\text{CO}_2$  contamination originating from the atmosphere, ' $f_{air}^{cb}$ ', and the  $^{14}\text{C}$  activity, ' $A_{air}$ ', were quantified by AMS and a series of parameters including excess air factor, air leakage coefficient of the air preheater, and the  $\text{CO}_2$  content in the flue gas. The quantification of ' $f_{air}^{cb}$ ' (0.23, 0.23, 0.225, 0.24, 0.25, 0.245, (%), respectively) was consistent with  $0.25 \pm 0.03\%$  presented in [15]. Surprisingly the  $^{14}\text{C}$  activity (98.24 pMC) of the sampling air which might be filled with fossil-derived  $\text{CO}_2$  was not substantially lower than the Northern Hemisphere atmosphere, which was probably due to the fast cycle of emitted flue gas with the atmosphere. The contamination from  $\text{CO}_2$  absorbed by NaOH was considered to be approximately equal to that occurring on the free-fall reactor experimental system because the period between the preparation and treatment of NaOH, and the sampling flow rate were identical to that in the laboratory. As the denominator in Eq. (4), ' $A_{biomass}$ ', affecting the accuracy of the ultimate results to a great extent, were analyzed by AMS which is more precise than LSC.

### 3.1.7. Blending ratios of two benchmarks

The carbon-based biomass-coal blending ratios obtained by the two  $^{14}\text{C}$ -based routes are summarized in Table 6. The carbon-based biomass-coal blending ratios presented in Table 6 were related to completely burned fuel, which was slightly larger than those calculated by ' $C_{loss}$ ', related to all fuel whether completely burned or not (2.94, 2.27, 2.39,

2.74, 3.38, 3.55, (%), respectively). The energy-based blending ratios of biomass, ' $f_{biomass}^{eb}$ ', calculated by Eq. (7) through ' $f_{biomass}^{cb}$ ' and ' $HC_{biomasscoal}$ ' (see Section 3.2.1), are shown in Fig. 5 together with ' $f_{biomass}^{eb-DCS}$ ' (the reference of energy-based biomass blending ratios calculated by the DCS). The reference, ' $f_{biomass}^{eb-DCS}$ ', calculated by the load of the gasifier in comparison to that of the pulverized coal furnace (representing the ratio of the electricity generated by biomass to the total power generation), was considered as a general reference for the biomass blending ratios.

Generally speaking, the results of LSC-benzene synthesis, AMS-graphitization, and the DCS reference values agreed well. When the kinds of biomass and coal or the actual blending ratios changed, the accuracy of the  $^{14}\text{C}$  method was not disturbed accordingly. When there was a slight change in the boiler load, i.e., a slight change in the biomass blending ratios, the  $^{14}\text{C}$  method could accurately and sensitively follow the trend of the change. The uncertainty of AMS-graphitization was lower than LSC-benzene synthesis as usual. It is worth mentioning that the DCS references of six operating conditions were all within the uncertainty range of LSC-benzene synthesis, which showed LSC-benzene synthesis was fully capable of satisfying the accuracy requirements in industrial sites.

The relative uncertainty of the LSC results ranged from 11.58% to 13.88%, which was consistent with the found in the studies at a wood-fired power plant located in Dutch [15] and the studies for the calculation of the biobased carbon content of liquid fuels [20]. The relative errors of the results were below 10.68% and the absolute errors were below 0.22%, when the blending ratios were below 3%. Within the operating conditions, IPP3, IPP5, and IPP6 results were more accurate; they had the absolute errors of 0.07%, 0.10%, and 0.12%, respectively. IPP1, IPP2, and IPP4 samples had slightly larger errors but within the acceptable ranges, which were probably ascribed to the errors of parameters used for calculation of ' $f_{biomass}^{eb}$ ' from ' $f_{biomass}^{cb}$ ' provided by the DCS. Thus, the carbon-based blending ratios of biomass, ' $f_{biomass}^{cb}$ ', straightforwardly reflecting the ratios of biogenic carbon participating in combustion to the total combusted carbon is more recommended than ' $f_{biomass}^{eb}$ ' which may be affected by the inaccuracy of operating parameters provided by the DCS.

### 3.1.8. Comparison of the two $^{14}\text{C}$ -based routes

Overall, the results of AMS-graphitization and LSC-benzene synthesis agreed excellently. The uncertainty of AMS was about ten times lower than that of LSC, which was due to the different measuring principles (one is the direct measurement of the quantity ratio of  $^{14}\text{C}$  and  $^{12}\text{C}$  while the other one is the indirect measurement through the scintillation frequency of scintillators), but the absolute and relative errors of two routes, as mentioned in 3.1.2, were not very different. Low sample requirements and a simple sample preparation cycle are the main advantages of AMS, but the obstacle to the popularization of AMS-graphitization is its expensive price, about ten times higher than LSC-benzene synthesis. From the experimental results, LSC-benzene synthesis method could fully satisfy the demand of the accuracy of the biomass-coal blending ratios in industrial power plants, therefore, it is more cost-effective than AMS-graphitization method.

**Table 4**

The operation parameters of biomass gasifier and pulverized coal furnace.

| Operating condition | Biomass gasifier |           |                        | Pulverized coal furnace |           |                |                     |
|---------------------|------------------|-----------|------------------------|-------------------------|-----------|----------------|---------------------|
|                     | Biomass          | Load [MW] | $HC_{biomass}$ [kJ/gC] | Coal                    | Load [MW] | $C_{loss}$ [%] | $HC_{coal}$ [kJ/gC] |
| IPP-1               | RH               | 11.36     | 29.17                  | Coal 1                  | 551.22    | 1.37           | 38.41               |
| IPP-2               | RH + CS          | 10.68     | 26.34                  | Coal 2                  | 579.47    | 1.75           | 36.42               |
| IPP-3               | RH + CS          | 11.18     | 28.00                  | Coal 3                  | 569.58    | 1.56           | 36.13               |
| IPP-4               | CS               | 11.29     | 28.07                  | Coal 3                  | 550.39    | 1.58           | 36.12               |
| IPP-5               | RH + BWR         | 10.47     | 27.20                  | Coal 4                  | 392.85    | 1.99           | 36.85               |
| IPP-6               | RH + BWR         | 10.93     | 27.38                  | Coal 4                  | 419.88    | 2.17           | 36.98               |

**Table 5**  
The key parameters of the  $^{14}\text{C}$  method in the industrial power plant.

| Operating condition | $A_{\text{fluegas}}$ [pMC] |                    | $f_{\text{air}}^{\text{cb}}$ [%] | $A_{\text{air}}$ [pMC] | $A_{\text{NaOH}} \times f_{\text{NaOH}}^{\text{cb}}$ [pMC] | $A_{\text{biomass}}$ [pMC] |
|---------------------|----------------------------|--------------------|----------------------------------|------------------------|--|----------------------------|
|                     | LSC-Benzene synthesis      | AMS-Graphitization |                                  |                        |  |                            |
| IPP-1               | 3.38 ± 0.44                | 3.30 ± 0.06        | 0.23                             | 98.24 0.59             | 0.19 ± 0.06  | 99.41 ± 0.62               |
| IPP-2               | 2.70 ± 0.41                | 3.02 ± 0.07        | 0.23                             |                        |  | 98.91 ± 0.59               |
| IPP-3               | 2.82 ± 0.45                | –                  | 0.225                            |                        |  | 98.91 ± 0.59               |
| IPP-4               | 3.17 ± 0.44                | 3.45 ± 0.07        | 0.24                             |                        |  | 98.37 ± 0.57               |
| IPP-5               | 3.87 ± 0.43                | 3.87 ± 0.08        | 0.25                             |                        |  | 99.68 ± 0.58               |
| IPP-6               | 4.06 ± 0.47                | –                  | 0.245                            |                        |  | 99.68 ± 0.58               |

**Table 6**  
The carbon-based blending ratios of biomass calculated by LSC-benzene synthesis and AMS-graphitization.

| Operating condition | $f_{\text{biomass}}^{\text{cb}}$ [%] |                    |
|---------------------|--------------------------------------|--------------------|
|                     | LSC-benzene synthesis                | AMS-graphitization |
| IPP-1               | 2.98 ± 0.45                          | 2.90 ± 0.09        |
| IPP-2               | 2.31 ± 0.41                          | 2.63 ± 0.09        |
| IPP-3               | 2.43 ± 0.46                          | –                  |
| IPP-4               | 2.79 ± 0.46                          | 3.07 ± 0.09        |
| IPP-5               | 3.45 ± 0.44                          | 3.45 ± 0.10        |
| IPP-6               | 3.63 ± 0.48                          | –                  |

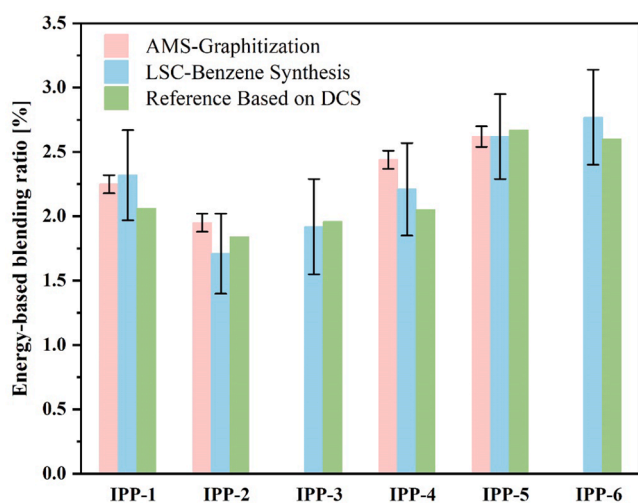


**Fig. 5.** The energy-based blending ratios of six operating conditions and their references.

### 3.2. Factors affecting the accuracy of the $^{14}\text{C}$ method

#### 3.2.1. Sampling

A significant aspect affecting the reasonableness of flue gas  $\text{CO}_2$  sampling, the main steps in the strategy, is whether the collected samples are representative during the period of biomass gas and coal co-combustion. A representative  $\text{CO}_2$  sample is not only the combustion product from the portion of the fuel to be measured (time homogeneity), but also the  $\text{CO}_2$  that should be uniformly distributed at different locations in the boiler flue (spatial homogeneity). Each operating condition lasted approximately three hours, and the  $\text{CO}_2$  sampling was scheduled for the middle hour, with the first hour of preparation and the last hour of sample processing. The rapidity of material circulation in power plant boilers made it reasonable to believe that this fraction of  $\text{CO}_2$  represented the fraction of combustion products to be measured. However, the spatial homogeneity of the sampled  $\text{CO}_2$  was, for the reason of the building structure of the power plant (only one site presented where the sampling can be performed safely), not be ensured. Due to the consistency of the final measurement and the DCS reference values, we believe

that the spatial distribution of  $\text{CO}_2$  was homogenous. Nevertheless, to avoid inhomogeneity of  $\text{CO}_2$  distribution from either biogas or coal in different sampling sites, multiple  $\text{CO}_2$  sampling at several sites is still recommended for future work. Another factor that might alter the reliability of flue gas  $\text{CO}_2$  sampling is the occurrence of leaks or blockages during the sampling interval, which may cause  $\text{NaOH}$  to absorb large amounts of ambient  $\text{CO}_2$ . In this study, all the interfaces were tightly sealed and the  $\text{O}_2$  and  $\text{CO}_2$  data from flue the gas analyzer monitored the unobstructed situation in real time.

The most appropriate ambient  $\text{CO}_2$  sampling location is where the air was pumped into the boiler, i.e., the inlet of the blower, because the purpose of air sampling is to deduct the contamination introduced by  $\text{CO}_2$  in the air as the combustion agent. There were six blowers providing air to the specific pulverized coal furnace, but the spacing of about ten meters among them gave us confidence that the air was evenly distributed in such a small space. Moreover, the air sampling was randomly carried out at different blowers during the six operating conditions, so the representative and uniform air  $\text{CO}_2$  were sampled.

The biomass and coal were simultaneously sampled at equal intervals from the furnace conveyor and analyzed after a strict quadrature in the laboratory. About 100 g fuel looked like somewhat insignificant and non-representative compared to the large amount of fuel fed into the boiler, especially for perennial biomass which might have the different  $^{14}\text{C}$  activities, because the  $^{14}\text{C}$  activity was affected not only by the growing location but also by the planting and harvest years [13]. Zhou et al. [32] found the  $^{14}\text{C}$  contents of samples from a road side in the downtown area and a public park were different, but no difference was found in the  $^{14}\text{C}$  activity for the different parts of corn straw, suggesting that there was not much difference existing in the  $^{14}\text{C}$  activities of biomass with the same origin on the conveyor belt at the period of several hours. However, we cannot accurately predict the  $^{14}\text{C}$  activity of pure biomass utilized by industrial power plants for the time being, so we still need the course of biomass collection and the  $^{14}\text{C}$  determination to ensure the accuracy of the results. The accurate prediction of the  $^{14}\text{C}$  activity of pure biomass could reduce the time cost and the economic cost of the metering scheme to a certain extent. Therefore, presenting an average reference of the  $^{14}\text{C}$  activity of pure biomass fuel, as the work of [17], is recommended.

#### 3.2.2. Selection of the $^{14}\text{C}$ test routes

From the results of experiments performed on the free-fall reactor, even though the precision of LSC-benzene synthesis was inferior to that of AMS-graphitization, it was fully capable of satisfying the accuracy requirements of the calculation of biomass-coal blending ratios based on the  $^{14}\text{C}$  method. In order to improve the economy, LSC was selected as the main route to the test of  $^{14}\text{C}$  activity of flue gas samples with AMS as the assisting method to verify the repeatability of the results. The  $^{14}\text{C}$  activity of pure biomass, ' $A_{\text{biomass}}$ ', as the denominator in the calculation equation, has a significant impact on the uncertainty of the ' $f_{\text{biomass}}^{\text{cb}}$ ', so the AMS was selected for the analysis of the  $^{14}\text{C}$  activity of the pure biomass. Due to the little content of atmospheric  $\text{CO}_2$ , the amount of air  $\text{CO}_2$  samples were very limited, so it could only be analyzed by AMS. Although the accurate results of blending ratios could be obtained by the two  $^{14}\text{C}$  test routes, both test routes required off-line sample preparation,

leading to a drawback that the metering scheme has not yet been able to complete online real-time monitoring of biomass-coal blending ratios.

### 3.2.3. Calculation formula

According to the formula, the accuracy of the calculated results depends not only on ' $A_{fluegas}$ ' and ' $A_{biomass}$ ', but also on the deductions of ' $A_{air} \times f_{air}^{cb}$ ' and ' $A_{NaOH} \times f_{NaOH}^{cb}$ ', which are the  $CO_2$  existing in the emitted flue gas but originating from other routes. Although ' $f_{air}^{cb}$ ' only accounts for about 0.25% [15], the high  $^{14}C$  activity of ambient  $CO_2$  about 100 pMC still leads to a large degree of  $^{14}C$  contamination, especially when the biomass-coal blending ratios are low. The carbon-based biomass-coal blending ratios calculated by LSC-benzene synthesis were 2.98, 2.31, 2.43, 2.79, 3.45, 3.63 (%), respectively, while the results were 3.21, 2.54, 2.65, 3.03, 3.69, 3.88 (%), respectively, if ' $A_{air} \times f_{air}^{cb}$ ' was not considered.

Compared with the contamination introduced by the combustion agent, the  $CO_2$  contamination introduced by NaOH absorption cannot be ignored, which might result in a relative error of about 6%–10%. In this study, the value of ' $A_{NaOH} \times f_{NaOH}^{cb}$ ' was taken as 0.19 pMC (the same as experiments carried out on free-fall reactor), which was far less than 2–4 pMC in previous studies [15,16]. This was because the  $CO_2$  dissolved by NaOH was immediately converted into dry  $SrCO_3$ , which cannot absorb ambient  $CO_2$  on the way back to the laboratory. Performing a  $CO_2$  dissolution and extraction of blank NaOH solution which is prepared simultaneously, not for absorbing flue gas  $CO_2$  but for accurately determining the value of ' $f_{NaOH}^{cb}$ ', is recommended in the future study.

## 4. Conclusion

To verify the accuracy and sensitivity of the  $^{14}C$  method applied in the determination of biomass-coal blending ratios, co-combustion experiments with blending ratios ranging from 0.99% to 10.93% were performed on the free-fall reactor in the laboratory. The absolute and relative errors of biomass-coal blending ratios calculated by the  $^{14}C$  method in the laboratory were less than 0.43% and 5.69%, based on which, a scheme for measuring biomass-coal blending ratios in industrial power plants was established and applied. Although the blending ratios in the power plant were below 3%, they were accurately metered by the scheme (less than 0.22%, 10.68% of absolute and relative errors). Great agreement between AMS and LSC showed LSC was sufficiently-accurate and cost-effective. Factors such as sampling and  $CO_2$ -contamination affecting the accuracy should be considered. This work provides a great opportunity for the future development of co-combustion.

### CRedit authorship contribution statement

**Yinchen Wang:** Conceptualization, Data curation, Formal analysis, Investigation, Methodology, Visualization, Writing – original draft, Writing – review & editing. **Zhongyang Luo:** Conceptualization, Funding acquisition, Methodology, Supervision, Validation. **Yuxing Tang:** Conceptualization, Data curation, Investigation. **Qinhui Wang:** Conceptualization, Funding acquisition. **Chunjiang Yu:** Resources, Supervision. **Xudong Yang:** Investigation. **Qianyuan Chen:** Investigation.

### Declaration of Competing Interest

The authors declare that they have no known competing financial interests or personal relationships that could have appeared to influence the work reported in this paper.

### Acknowledgements

This work was funded by the National Natural Science Foundation of China and U.S. National Science Foundation, namely, NSFC-NSF project (Grant NO. 51661125012).

## Appendix A. Supplementary data

Supplementary data to this article can be found online at <https://doi.org/10.1016/j.fuel.2022.125198>.

## References

- [1] Jia Z, Lin B. How to achieve the first step of the carbon-neutrality 2060 target in China: The coal substitution perspective. *Energy* 2021;233:121179.
- [2] Shan F, Lin Q, Zhou K, Wu Y, Fu W, Zhang Po, et al. An experimental study of ignition and combustion of single biomass pellets in air and oxy-fuel. *Fuel* 2017; 188:277–84.
- [3] Li J, Yang W, Blasiak W, Ponzio A. Volumetric combustion of biomass for  $CO_2$  and  $NO_x$  reduction in coal-fired boilers. *Fuel* 2012;102:624–33.
- [4] Mlonka-Mędrala A, Magdziarz A, Kalembe-Rec I, Nowak W. The influence of potassium-rich biomass ashes on steel corrosion above 550 °C. *Energy Convers Manage* 2019;187:15–28.
- [5] Zhang H, Yu C, Luo Z. Investigation of ash deposition dynamic process in an industrial biomass CFB boiler burning high alkali and chlorine fuel. *RSC Adv* 2020; 10(36):21420–6.
- [6] Zhou H, Zhang H, Li L, Zhou B. Ash Deposit Shedding during Co-combustion of Coal and Rice Hull Using a Digital Image Technique in a Pilot-Scale Furnace. *Energy Fuels* 2013;27(11):7126–37.
- [7] Bhuiyan AA, Naser J. CFD modelling of co-firing of biomass with coal under oxy-fuel combustion in a large scale power plant. *Fuel* 2015;159:150–68.
- [8] Qiu S, Cai L. Recent advancement in radiocarbon dating. *Quaternary Sciences* 1997.
- [9] Guo X, Li P, Li H, Guo X, Bai H, Lv Q, et al. Determination of the bio-based content of bio-based plastics by liquid scintillation counting. *Chinese Journal of Analysis Laboratory* 2014.
- [10] Deng K, Ma Y, Wang H, Shen J, Tan W. Identification of the Bio-based and Petroleum Based Foam. *Chem Indus For Prod* 2016.
- [11] Norton GA, Hood DG, Devlin SL. Accuracy of radioanalytical procedures used to determine the biobased content of manufactured products. *Bioresour Technol* 2007;98(5):1052–6.
- [12] Hämäläinen KM, Jungner H, Antson O, Räsänen J, Tormonen K, Roine J. Measurement of Biocarbon in Flue Gases Using  $^{14}C$ . *Radiocarbon* 2007;49(2): 325–30.
- [13] Mohn J, Szidat S, Fellner J, Rechberger H, Quartier R, Buchmann B, et al. Determination of biogenic and fossil  $CO_2$  emitted by waste incineration based on  $(^{14}C)^{(2)}$  and mass balances. *Bioresour Technol* 2008;99(14):6471–9.
- [14] Mohn J, Szidat S, Zeyer K, Emmenegger L. Fossil and biogenic  $CO_2$  from waste incineration based on a yearlong radiocarbon study. *Waste Manag* 2012;32(8): 1516–20.
- [15] Palstra SW, Meijer HA. Carbon-14 based determination of the biogenic fraction of industrial  $CO_2$  emissions - application and validation. *Bioresour Technol* 2010; 101(10):3702–10.
- [16] Calcagnile L, Quarta G, D'Elia M, Ciceri G, Martinotti V. Radiocarbon AMS determination of the biogenic component in  $CO_2$  emitted from waste incineration. *Nucl Instrum Methods Phys Res, Sect B* 2011;269(24):3158–62.
- [17] Fellner J, Rechberger H. Abundance of  $(^{14}C)$  in biomass fractions of wastes and solid recovered fuels. *Waste Manag* 2009;29(5):1495–503.
- [18] Fuglsang K, Pedersen NH, Larsen AW, Astrup TF. Long-term sampling of  $CO_2$  from waste-to-energy plants:  $(^{14}C)$  determination methodology, data variation and uncertainty. *Waste Manag Res* 2014;32(2):115–23.
- [19] Kang S, Cha JH, Hong YJ, Lee D, Kim KH, Jeon EC. Estimation of optimal biomass fraction measuring cycle for municipal solid waste incineration facilities in Korea. *Waste Manag* 2018;71:176–80.
- [20] Haverly MR, Fenwick SR, Patterson FPK, Slade DA. Biobased carbon content quantification through AMS radiocarbon analysis of liquid fuels. *Fuel* 2019;237: 1108–11.
- [21] Doll CG, Plymale AE, Cooper A, Kutnyakov I, Swita M, Lemmon T, et al. Determination of low-level biogenic gasoline, jet fuel, and diesel in blends using the direct liquid scintillation counting method for  $^{14}C$  content. *Fuel* 2021;291: 120084.
- [22] Palstra SWL, Meijer HAJ. Biogenic Carbon Fraction of Biogas and Natural Gas Fuel Mixtures Determined with  $^{14}C$ . *Radiocarbon* 2016;56(1):7–28.
- [23] Tang Y-X, Luo Z-Y, Yu C-J, Cen J-M, Chen Q-Y, Zhang W-N. Determination of biomass-coal blending ratio by  $^{14}C$  measurement in co-firing flue gas as  $^{14}C$  法为基础的共燃烟气中生物质与煤的掺混比例测定方法. *Journal of Zhejiang University-SCIENCE A* 2019;20(7):475–86.
- [24] Quarta G, Ciceri G, Martinotti V, D'Elia M, Calcagnile L. Bringing AMS radiocarbon into the Anthropocene: Potential and drawbacks in the determination of the bio-fraction in industrial emissions and in carbon-based products. *Nucl Instrum Methods Phys Res, Sect B* 2015;361:521–5.
- [25] Jones FC, Blomqvist EW, Bisaillon M, Lindberg DK, Hupa M. Determination of fossil carbon content in Swedish waste fuel by four different methods. *Waste Manag Res* 2013;31(10):1052–61.
- [26] Muir GKP, Hayward S, Tripney BG, Cook GT, Naysmith P, Herbert BMJ, et al. Determining the biomass fraction of mixed waste fuels: A comparison of existing industry and  $(^{14}C)$ -based methodologies. *Waste Manag* 2015;35:293–300.
- [27] Yang W, Ni Y, Lei H. Biomass direct coupled combustion power generation technology for coal fired power station: a review. *Thermal Power Generation* 2021.

- [28] Xu X, Trumbore SE, Zheng S, Southon JR, McDuffee KE, Luttgen M, et al. Modifying a sealed tube zinc reduction method for preparation of AMS graphite targets: Reducing background and attaining high precision. *Nucl Instrum Methods Phys Res, Sect B* 2007;259(1):320–9.
- [29] Mook WG, van der Plicht J. Reporting  $^{14}\text{C}$  Activities and Concentrations. *Radiocarbon* 2016;41(3):227–39.
- [30] Levin I, Kromer B. The Tropospheric  $^{14}\text{C}$  Level in Mid-Latitudes of the Northern Hemisphere (1959–2003). *Radiocarbon* 2016;46(3):1261–72.
- [31] Tang Y, Luo Z, Yu C. Accuracy Improvement of the  $^{14}\text{C}$  Method Applied in Biomass and Coal Co-Firing Power Stations. Accuracy Improvement of the  $^{14}\text{C}$  Method Applied in Biomass and Coal Co-Firing Power Stations 2021;9(6):994.;9(6):994.
- [32] Zhou W, Wu S, Huo W, Xiong X, Cheng P, Lu X, et al. Tracing fossil fuel  $\text{CO}_2$  using  $\Delta^{14}\text{C}$  in Xi'an City. *China Atmospheric Environment* 2014;94:538–45.